processes

MDPI

Article

The Effect of Water–Rock Interaction on Shale Reservoir Damage and Pore Expansion

Jin Pang *, Tongtong Wu, Xinan Yu, Chunxi Zhou, Haotian Chen and Jiaao Gao

School of Petroleum and Gas Engineering, Chongqing University of Science and Technology, Chongqing 401331, China; 2024201059@cqust.edu.cn (J.G.)
* Correspondence: 2006054@cqust.edu.cn

Abstract: This study investigates the microscopic structural changes and the evolution of physical properties in typical shale samples from three wells in southwestern China during water–rock interactions. Using scanning electron microscopy (SEM), nuclear magnetic resonance (NMR), and other techniques, we analyzed the changes in pore structure, mineral dissolution behavior, and fracture propagation in shale samples of different types (organic-rich, mixed, and inorganic) during water immersion. The results show that water–rock interaction significantly affects the porosity, fracture width, and physical properties of shale. As the reaction time increases, the pore volume and number of pores generally increase in all shale types, with significant fracture propagation. Furthermore, fracture width changes exhibit varying trends depending on the reaction depth. NMR T2 spectrum analysis indicates that water–rock interaction not only influences the expansion of microfractures but also shows different responses in organic and inorganic pores. SEM images further reveal the impact of water–rock interaction on mineral dissolution, particularly during the early stages, where the dissolution of minerals significantly alters the pore structure. Overall, water–rock interaction plays a crucial role in the development of shale gas reservoirs, providing valuable data and theoretical support for future shale gas extraction.

Keywords: water–rock interaction; shale pore structure; nuclear magnetic resonance and scanning electron microscope; porosity and fracture propagation

Academic Editor: Qingbang Meng

Received: 31 March 2025
Revised: 16 April 2025
Accepted: 21 April 2025
Published: 22 April 2025

Citation: Pang, J.; Wu, T.; Yu, X.; Zhou, C.; Chen, H.; Gao, J. The Effect of Water–Rock Interaction on Shale Reservoir Damage and Pore Expansion. *Processes* **2025**, *13*, 1265. https://doi.org/10.3390/pr13051265

1. Introduction

Shale gas, as an important unconventional natural gas resource, has attracted much attention due to its abundant reserves and clean and efficient characteristics. The core feature of shale gas reservoirs lies in their extremely low porosity (usually <10%) and nanoscale permeability (<0.1 mD), resulting in the coexistence of gas in both adsorbed (adsorbed on the surface of organic matter) and free (residing in microfractures and pores) states [1–3]. This dual storage mechanism results in the migration pattern of shale gas being significantly different from that of conventional gas reservoirs. Economic exploitation of shale gas requires the creation of a complex fracture network through artificial fracturing. In addition, the mineral composition of shale (such as high clay content or the proportion of brittle minerals) directly affects the reservoir's frackability, while the organic matter abundance (TOC) and maturity (Ro) determine the hydrocarbon generation capacity and adsorbed gas content.

With the rapid development of shale gas production, the water–rock interaction in shale gas reservoirs has become one of the primary areas of research. Water–rock interaction not only directly affects the pore structure, fracture propagation, and physical properties of

shale reservoirs but also plays a crucial role in the extraction of shale gas [4]. The reservoir characteristics of shale gas are primarily determined by its porosity, permeability, and microstructure, all of which are significantly influenced by water–rock interaction [5–7]. Therefore, in-depth studies of the microstructural changes of shale under water–rock interaction are of great theoretical significance and practical value for understanding shale gas accumulation and extraction mechanisms.

Currently, academic research on water–rock interaction mainly focuses on pore evolution, mineral dissolution, and fracture propagation in shale. Some studies have investigated the changes in pore characteristics and the short-term effects of water–rock interaction in shale gas reservoirs. For example, Zhou et al. [8] used nuclear magnetic resonance (NMR) technology to study changes in shale porosity under different water–rock interactions, revealing the significant influence of water–rock interaction on shale pore structures and pointing out that it is a key factor affecting the physical property changes of shale reservoirs. Similarly, Liu et al. [9] studied the evolution of pore structures in shale under a water medium, finding that water–rock interaction not only increases pore volume but also affects fracture propagation and pore connectivity. Phan et al. [10] experimentally explored the water–rock reaction process of shale samples under different water chemical conditions, emphasizing the importance of water–rock interaction in shale gas extraction. Zhou et al. [11] analyzed the effects of water–rock reactions on shale porosity and fracture propagation using SEM and NMR, summarizing the short-term evolution patterns of shale gas permeability and pore structures due to water–rock interaction. Additionally, Goodman et al. [12] investigated the mineral dissolution behavior in water–rock reactions, revealing the impact of different mineral components on the reaction process.

In other aspects, Fabián et al. [13] investigated the fluid–rock interaction processes in ancient subduction zones, revealing the transport and reaction of fluids in subduction zones and their impacts on the physicochemical properties of rocks, which is of great significance for understanding the material circulation and energy transformation in subduction zones. John et al. [14] studied the migration of trace elements in subduction slabs caused by unsteady fluid–rock interactions, providing important information for understanding element cycling in hydrothermal systems. Simon et al. [15] studied the high pore pressure and porosity at a depth of 35 km in the Cascadia subduction zone, emphasizing the geological record of water–rock interactions in the deep subduction zone. Taetz et al. [16] investigated the fluid–rock interactions and their evolution in high-pressure/low-temperature veins in eclogites, revealing the transport paths and reaction mechanisms of fluids in rocks.

These studies have deepened our understanding of the influence of water–rock interaction on shale gas reservoirs and provided theoretical foundations for shale gas development. Despite extensive research on the effects of water–rock interaction on shale physical properties, most studies are limited to short-term experimental scales, and the differences in the responses of different shale types to water–rock interaction have not been systematically compared and summarized. In addition, existing studies have mostly focused on a single type of shale, lacking a comprehensive comparison of the microstructural changes in organic-rich, mixed, and inorganic shales under water–rock interaction. Therefore, this study selected typical shale samples (Z8, Z3, and Z7) from three wells in southwestern China and used SEM, NMR, and other methods to thoroughly investigate the effects of water–rock interaction on the microstructure and physical properties of different shale types.

2. Materials and Methods

2.1. Sample Collection and Preparation

This study selected three different shale samples (Z8, Z3, and Z7) from three wells in southwestern China (Zu 201 Well, Longmaxi Formation, Western Chongqing Block, Dazu District, Chongqing, China, 105°52′30.38″ east longitude, 29°40′33.53″ north latitude), representing typical characteristics of organic-rich, mixed (organic–inorganic), and inorganic shale types. To ensure the accuracy and reliability of experimental data, the samples were first dried to remove surface moisture. Subsequently, the samples were finely cut and ground according to the experimental requirements, to provide suitable materials for subsequent SEM, NMR, and ion exchange experiments.

2.2. Water–Rock Interaction Experiment

The water–rock interaction experiment utilized a standard immersion method, aiming to systematically study the reaction characteristics of shale samples in an aqueous medium [17–19]. During the experiment, each sample was immersed in deionized water for 1, 3, 7, and 14 days to simulate water–rock interaction over different time scales. At the designated time points, the samples were extracted and analyzed using a series of characterization methods, including SEM, NMR, and ion exchange experiments. These analyses evaluated the changes in pore structure, mineral dissolution behavior, and fracture propagation under different immersion times. The aim was to reveal the impact of water–rock interaction on shale pore evolution, mineral composition, and physical properties, thereby providing important experimental data and theoretical support for the development and optimization of shale gas reservoirs.

2.3. Scanning Electron Microscopy (SEM)

SEM (Carl Zeiss AG, Oberkochen, Germany) was used to observe the microstructure of the shale samples to analyze changes in pores, fractures, and mineral dissolution during water–rock interaction [20]. SEM images provided direct representation of the effects of water–rock interaction on mineral dissolution mechanisms and pore expansion. Specifically, image analysis revealed the mineral dissolution behavior induced by water–rock reactions and its impact on pore structure evolution, allowing the exploration of how water–rock interaction alters shale microstructures under different conditions [21–23]. By comparing SEM images taken at different immersion time points, we were able to identify trends in the evolution of shale microstructures over time, providing theoretical insights into the long-term impact of water–rock interaction on shale physical properties.

2.4. Nuclear Magnetic Resonance (NMR)

In this study, NMR (Oxford Instruments Technology Co., Ltd., Shanghai, China) experiments were conducted using T2 relaxation time spectra to accurately determine the distribution of pores in shale samples. T2 spectra taken at different time points revealed the evolution and changes in pore structure during water–rock interaction [24]. Specifically, T2 spectra provided important information on pore expansion and fracture development, especially in the presence of water–rock interaction, where the enlargement of microfractures and pores was effectively reflected. By comparing T2 relaxation time spectra at different immersion time points, we analyzed the impact of water–rock reactions on the shale microstructure and explored the long-term evolution of physical properties in shale reservoirs [25]. This analysis not only provided theoretical foundations for understanding the mechanisms of water–rock interaction in shale reservoirs but also offered crucial data support for predicting trends in porosity and permeability during shale gas development.

3. Results

3.1. NMR T2 Spectrum Characteristics

NMR T2 spectrum analysis comparing the experimental results of oil and water absorption revealed changes in pore volume, pore quantity, and fracture propagation during water–rock reactions.

The T2 spectrum morphology reflects the distribution of pores and fracture structures within the core. A larger transverse relaxation time in the T2 spectrum indicates larger pore or fracture sizes. Based on the literature and experimental data, transverse relaxation times greater than 100 ms correspond to the response characteristics of microfractures. The integral area of the T2 spectrum is proportional to the amount of fluid in the rock and reflects changes in porosity. The variation in the integral area directly corresponds to changes in pore volume and quantity.

(1) T2 Spectrum Characteristics of Different Pore Types

Oil-imbibition T2 spectra: These primarily reflect the characteristics of organic pores in the reservoir. Peaks at smaller relaxation times (1–10 ms) indicate well-developed organic pores with larger diameters and volumes.

Water-imbibition T2 spectra: These primarily reflect the characteristics of inorganic pores and fractures. After water imbibition, the response at T2 > 100 ms intensifies, indicating a more significant impact of water on larger pores and fractures (Figure 1).

(2) T2 Spectrum Changes for Different Pore Types During Water–Rock Interaction

Organic pore–fracture type: The main peak of the oil-imbibition T2 spectrum appears in the 1–10 ms range, indicating well-developed pores with large volumes. After water imbibition, the main peak shifts to 0.1–1 ms, suggesting smaller pore diameters and enhanced interaction between water and inorganic pores (Figure 1a).

Organic–inorganic pore–fracture type: The main peak of the oil-imbibition T2 spectrum is located near 0.1 ms, reflecting small pore diameters but high total pore volume. After water imbibition, the main peak shifts to >1 ms, indicating further enhancement of water's effect on inorganic pores (Figure 1b).

Inorganic pore–fracture type: Organic pores are poorly developed. After water imbibition, pore diameter and volume increase, and the T2 spectrum peak is located in the 1–10 ms range, reflecting a significant effect of water–rock interaction on inorganic pores (Figure 1c).

(3) Influence of Water–Rock Interaction on T2 Spectrum

Changes in T2 spectra from dry samples to those exposed to water–rock interactions reveal that the area of the spectrum peaks at <10 ms gradually increases, and the main peak shifts to larger T2 values. This indicates increases in porosity and pore volume. A similar trend is observed for the spectral peaks at T2 > 100 ms (Figure 1).

In the early stages of water–rock interaction (within 22 h), pore volume and diameter grow rapidly, particularly in organic pore–fracture types, where fracture volume expansion is significant. As the interaction progresses (120 h), the growth in pore volume slows for different pore types, but the number of fractures continues to increase (Figure 1).

(4) Change in Fracture Porosity

The T2 spectral components at T2 > 100 ms represent fracture porosity.

For the organic pore–fracture type, fracture porosity increases from 0.30% (oil imbibition) to 0.78% (water imbibition), an increase of 160%.

For the organic–inorganic pore–fracture type, fracture porosity increases from 0.18% (oil imbibition) to 0.43% (water imbibition), an increase of 139%.

For the inorganic pore–fracture type, fracture porosity increases from 0.071% (oil imbibition) to 0.10% (water imbibition), an increase of 41% (Figure 1).

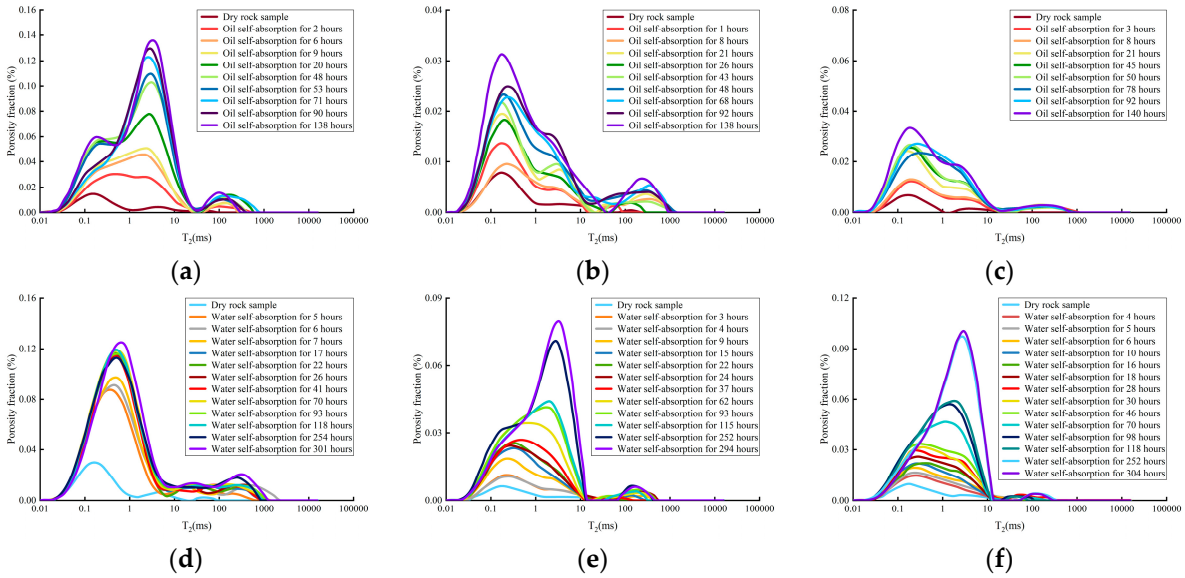

Figure 1. T2 spectral characteristics of shale samples during oil and water imbibition at different time intervals. (**a**) Organic pore–fracture type, oil imbibition; (**b**) organic–inorganic pore–fracture type, oil imbibition; (**c**) inorganic pore–fracture type, oil imbibition; (**d**) organic pore–fracture type, water imbibition; (**e**) organic–inorganic pore–fracture type, water imbibition; (**f**) inorganic pore–fracture type, water imbibition.

3.2. Scanning Electron Microscope Observation Characteristics

(1) Organic Pore Change

SEM results (Figure 2) indicate that organic matter in the Z7 shale samples is distributed in blocks or dots, with low porosity. Organic pores are mostly nanoscale and elongated, with larger pores located in the center of the organic matter and smaller pores near the edges. Before and after water–rock interaction, the morphology, size, and position of the organic matter remain relatively unchanged. Larger organic pores remain stable, while smaller ones shrink or close, primarily along the edges of organic matter. This phenomenon occurs because water cannot effectively penetrate larger pores, and smaller pores tend to adsorb dissolved minerals, leading to their closure.

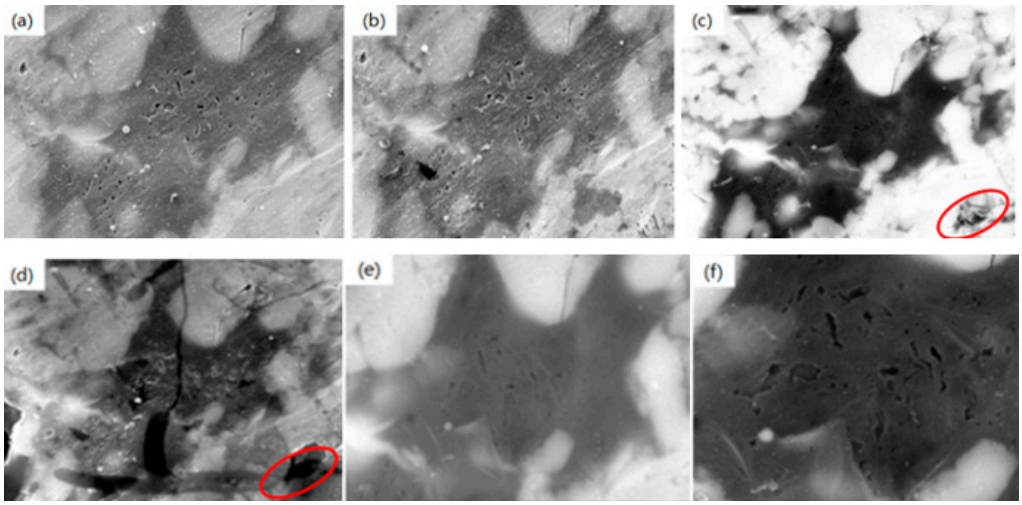

Figure 2. Evolution of organic pore structures in Z7 shale samples during water–rock interaction. (**a**) Before interaction; (**b**) day 1; (**c**) day 3; (**d**) day 7; (**e**) day 14; (**f**) magnified view, day 14.

(2) Inorganic Pore Space and Mineral Dissolution Changes

SEM results (Figure 3) show significant changes in Z7 samples during water–rock interaction. In the early stage (1 day), pore enlargement occurs without significant changes in pore diameter. Between 3 and 7 days, soluble minerals dissolve progressively, resulting in larger pores, complete dissolution of some minerals, and increased fracture size and number. By day 14, pore and fracture growth slows, but dissolution continues, further improving connectivity. These observations demonstrate that water–rock interaction significantly alters the pore structure and fracture network, enhancing porosity and connectivity.

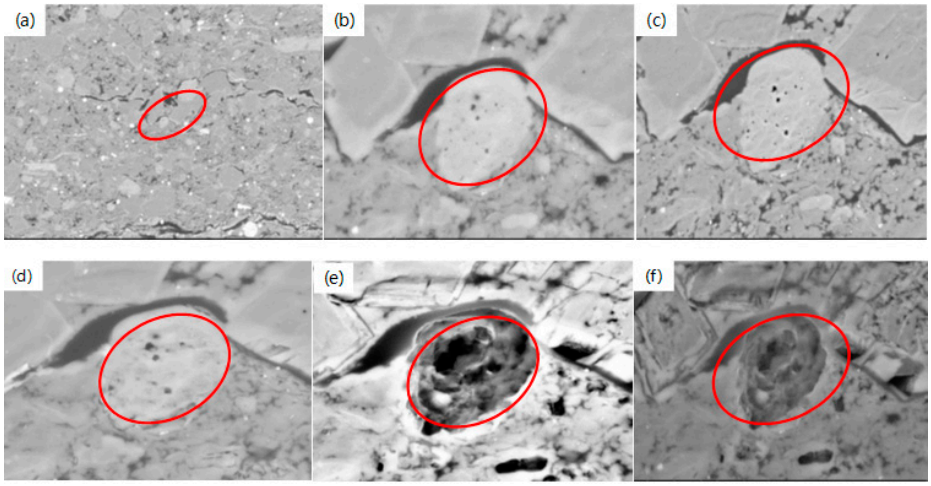

Figure 3. Evolution of dissolution pores in Z7 shale samples during water–rock interaction. (**a**) Before interaction; (**b**) pre-existing dissolution pores; (**c**) day 1; (**d**) day 3; (**e**) day 7; (**f**) day 14.

(3) Microcrack Change

SEM observations (Figure 4) indicate notable changes in microfractures during water–rock interaction in Z7 samples. Before the reaction, fracture widths range from 500 nm to 1 μm and are evenly distributed. After 1 day, fracture width increases by ~1.5 times, though mineral dissolution is not yet significant. By day 3, fracture propagation slows, and some microfractures are partially blocked by dissolved material. By day 14, fracture width increases to ~2.5 times its initial value, with significant fracture propagation. Overall, microfracture expansion intensifies with time, accompanied by gradual filling of some fractures with dissolved material.

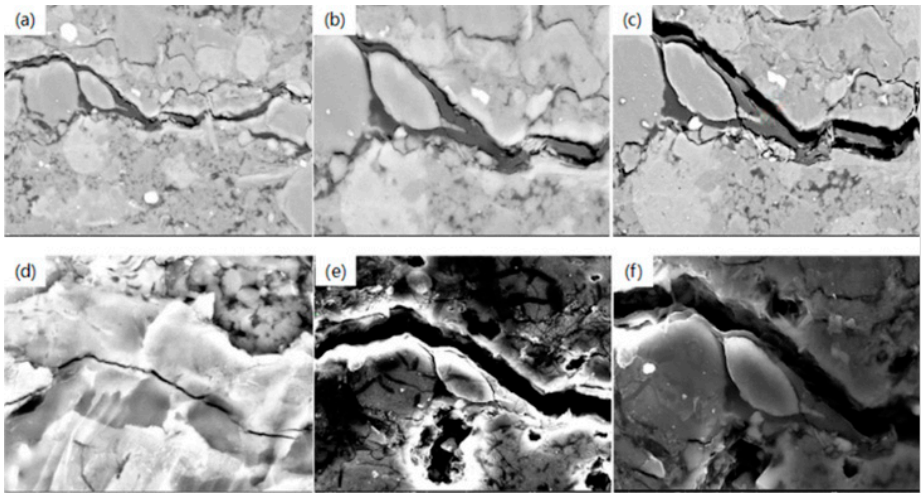

Figure 4. Evolution of microfractures in Z7 shale samples during water–rock interaction. (**a**) Before interaction; (**b**) microfractures before interaction; (**c**) day 1; (**d**) day 3; (**e**) day 7; (**f**) day 14.

3.3. Characteristics of Changes in Physical Parameters

During water–rock interaction, physical parameters such as fracture width, surface porosity, and overall porosity exhibit distinct trends over time (Figure 5).

Fracture width: In the early stages (1–3 days), fracture width increases across all samples, with the most rapid growth observed in Z8 samples. For Z3 and Z7 samples, the fracture width initially increases but later decreases. In the later stages (7–14 days), fracture widths in Z8 and Z7 samples peak by day 7 before shrinking, with Z7 samples exhibiting more pronounced reductions. In contrast, the fracture width in Z3 samples continues to expand gradually after day 7.

Surface porosity: Surface porosity increases significantly with prolonged water–rock interaction. For Z3 samples, early increases (1–4 days) are primarily driven by fracture propagation, while later increases (4–7 days) result from higher pore numbers and diameters. In Z7 samples, surface porosity growth during the first 7 days is influenced by both pores and fractures, but later increases are dominated by pore changes as fractures begin to fill. For Z8 samples, surface porosity changes remain relatively stable and are consistently influenced by both pores and fractures.

Porosity: Porosity increases steadily with time. In the early stages (1–4 days), porosity grows rapidly due to the increase in pore number and diameter. During the mid-stage (4–7 days), porosity growth slows but remains positive. In the later stages (7–14 days), growth slows further, with contributions primarily from changes in pore type and improved connectivity, especially as fractures are filled.

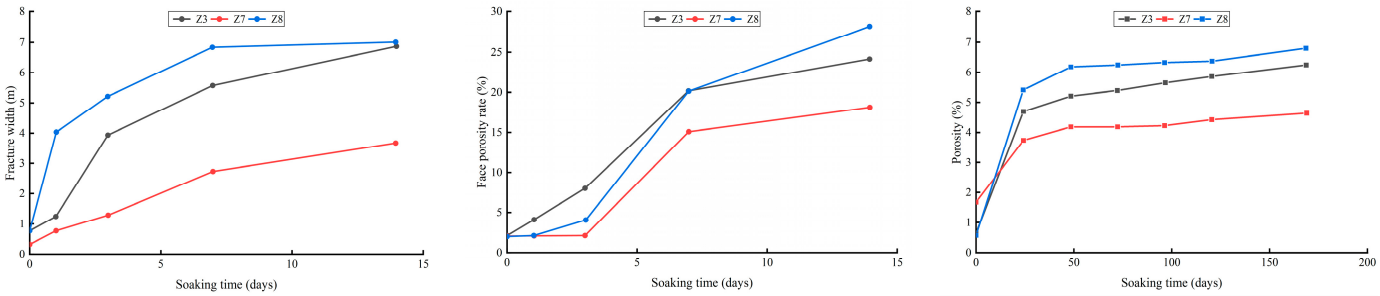

Figure 5. Relationships between physical parameters and soaking time for shale samples. (**a**) Fracture width vs. time; (**b**) surface porosity vs. time; (**c**) porosity vs. time.

4. Discussion

4.1. Change in Pore Structure and Increase in Porosity

Changes in inorganic pores: During the water–rock reaction process, the dissolution of soluble minerals leads to an increase in inorganic pores and porosity. As the reaction continues, the dissolution effect gradually strengthens, improving the connectivity of pores, which is beneficial to the extraction of shale gas. Zhou et al. [26] conducted water–rock interaction experiments considering reservoir water level fluctuations, taking the slightly weathered red-bed soft rock in the Three Gorges Reservoir area as the research object, and measured and analyzed the corresponding pore structure parameters. The study shows that the pore size gradually increases. During the 12 cyclic processes, the maximum pore diameter and average pore diameter of the rock samples increased by 101.02% and 43.32%, respectively, the porosity increased by 26.59%, while the number of pores decreased by 22.65%. Moreover, the water–rock interaction caused the pores to change from flat-oval to elongated shapes. This is consistent with the viewpoint in this study that water–rock reactions enhance the porosity and connectivity of inorganic pores, with both emphasizing

the impact of changes in inorganic pores during the reaction process on the performance of shale.

Expansion of microfractures: Water–rock reactions significantly promote the expansion of microfractures, especially in the early stages of the reaction, when the width of the fractures increases rapidly. As the water–rock reaction proceeds, the speed of fracture expansion gradually slows down, but the number and width of fractures continue to increase, indicating that the effect of the water–rock reaction is gradually stabilizing. Jiang et al. [5] demonstrated through experiments that water–rock interaction can activate and extend natural fractures. During the spontaneous imbibition process, the rock permeability can increase by 20.0–61.6%. This indicates that water–rock reactions play a significant role in the extension of microfractures and the enhancement of rock permeability, which is consistent with the conclusions of this study regarding microfracture extension. Both highlight the important impact of water–rock reactions on shale microfractures.

4.2. Differences in Response of Pore Types to Water–Rock Reactions

Organic pore–fracture reservoirs: Water–rock reactions have a significant impact on the porosity and fracture volume of organic pore–fracture reservoirs, especially in the early stages of the reaction, when the pore volume and fracture volume increase rapidly. This indicates a strong pore–fracture relationship between organic pores and fractures, and the effect of hydration is strong, thereby promoting more effective fracture propagation. This reaction characteristic is helpful to improve the permeability of the reservoir and has important significance in the application of technologies such as hydraulic fracturing.

Inorganic pore–fracture reservoirs: In contrast, the impact of water–rock reactions on inorganic pore–fracture reservoirs is relatively mild. Although the porosity has increased, the effect of fracture propagation is weak, indicating that inorganic pores play a smaller role in water–rock reactions. This indicates that for inorganic pore reservoirs, other means (such as acidification treatment) may be needed to further enhance pore expansion and fracture connectivity.

Chen et al. [27] classified the pore–fracture structures and revealed their influence on hydraulic fracture propagation through physical simulation experiments. It was pointed out that in marine shale, the pore–fracture structures are mainly controlled by factors such as organic hydrocarbon generation, providing certain theoretical support for the study of the pore structure of organic pore–fracture reservoirs and the impact of water–rock reactions.

4.3. Damage to Pore Structure Caused by Water–Rock Reaction

Changes in organic pores: The impact of water–rock reactions on organic pores is relatively small; particularly, the effect on larger pores is not obvious. However, hydration mainly affects smaller organic pores, and during the reaction process, adsorptive hydration causes the closure of small pores. This phenomenon indicates that the impact of water–rock reactions on organic matter pores is mainly reflected in the changes in smaller pores, while the impact on larger pores is more limited. In some studies on coalbed methane reservoirs, Wang et al. [28] found that the influence of water–rock interaction on the organic pores in coal also exhibits a similar pattern, mainly affecting the micropores.

Mineral dissolution: The dissolution of minerals in water–rock reactions may lead to the dissolution of some soluble minerals, thereby changing the pore structure. As the reaction proceeds, the erosion of insoluble minerals gradually intensifies, and some pores and fractures may undergo further dissolution, increasing the width and number of fractures. This helps to improve the connectivity of the reservoir, but it may also cause local damage to the reservoir to a certain extent. Zhou et al. [29] analyzed the element dissolution characteristics of granite and gabbro under different thermal treatment temperatures. They

found that water–rock reactions lead to the dissolution of minerals in rocks, which in turn affects the microstructure and mechanical properties of the rocks. This is similar to the mechanism by which water–rock reactions cause mineral dissolution in shale gas reservoirs.

4.4. The Impact of Water–Rock Reaction on Shale Gas Extraction

Water–rock reactions significantly enhance the porosity and connectivity of fractures, thereby improving the permeability of shale reservoirs and providing favorable conditions for shale gas extraction. Water–rock reactions are particularly important in the early stages of the reservoir, where rapid increases in porosity and fractures can effectively enhance gas recovery rates. Chen et al. [30] proposed that water–rock reactions enhance permeability by causing microcracks in shale to expand and interconnect through hydration expansion. However, other studies have suggested that water–rock reactions may improve permeability by altering the microscopic structure of shale, such as dissolving mineral particles and generating new pores and fractures. Jia et al. [31] investigated the effects of injection rate, aqueous phase, and viscosity ratio. The results show that increasing the viscosity of the injected water can delay the breakthrough time, thereby enhancing the recovery efficiency.

4.5. The Actual Methods of Shale Gas Extraction

Given that water–rock interaction significantly enhances the porosity and permeability of shale, especially during the initial stages of the reaction, a targeted water injection strategy can be employed to maximize these benefits. For instance, injecting water into specific areas that are rich in organic matter or have high mineral dissolution potential can accelerate the development of microfractures and improve gas flow pathways.

Research has shown that the initial stage of water–rock interaction is crucial for the rapid development of pores and fractures. Therefore, optimizing the water injection rate can ensure sufficient time for water–rock reactions to occur while avoiding excessive pressure buildup. This approach can prevent premature fracture closure and ensure effective permeability enhancement.

Combining hydraulic fracturing with chemical additives that promote specific water–rock interactions can significantly enhance the effect. For example, using acids or chelating agents targeting specific minerals (such as carbonates or clays) can enhance the dissolution process, thereby creating more pathways for gas migration. This technique is particularly effective in carbonate-rich shale.

Adopting a stepwise production enhancement method, which involves initial hydraulic fracturing followed by controlled water injection to promote water–rock interaction, can optimize the fracture network. This method ensures that newly formed fractures are further strengthened through natural water–rock reactions, thereby improving the overall efficiency of gas extraction.

5. Conclusions

The interaction between water and rock has a significant impact on the pore structure of shale, especially in terms of inorganic pores and microfracture propagation. During the reaction process, the porosity increases, mainly manifested as the expansion of inorganic pore volume and the widening of fracture widths. This is attributed to the dissolution of soluble minerals, which enhances the number, size, and connectivity of pores, thereby improving the permeability and gas storage capacity of the shale. However, this effect varies depending on the pore type. In the early stage of the reaction, the volume of pores and fractures increases rapidly, while in the later stage, the growth tends to level off, although the number of fractures continues to increase. This influence is time-dependent and pore-

type-dependent, particularly in the case of inorganic pores, which can significantly enhance the permeability and gas storage capacity of shale, creating favorable conditions for shale gas extraction.

Future research should further explore the effects of different fluid compositions (such as saline water, acidic, or alkaline solutions) on shale–water–rock reactions to more accurately simulate actual reservoir conditions. Investigations should be performed regarding the coupling effects of fluid flow and pressure changes on water–rock reactions by using dynamic experiments to simulate the fluid flow environment during actual extraction processes. Experimental cycles should be extended to study the long-term evolution of shale microstructure and physical properties due to prolonged water–rock reactions. Numerical simulation methods, combined with experimental data, should be employed to predict the long-term impact of water–rock reactions on the performance of shale reservoirs.

Author Contributions: Conceptualization, J.P.; methodology, J.P.; formal analysis, H.C.; investigation, C.Z.; resources, J.P.; data curation, J.G.; writing—original draft preparation, T.W.; writing—review and editing, T.W.; supervision, X.Y.; project administration, X.Y. All authors have read and agreed to the published version of the manuscript.

Funding: This work was supported by the Chongqing Municipal Science and Technology Bureau Project Basic Research and Frontier Exploration Project "Study on Fracture Seepage Law of Interlayer Mixed Shale and Reservoir Selection" [grant numbers CSTB2023NSCQ-MSX0679] and the National Natural Science Foundation "Study on the Mechanism of Fracture Network Formation during Shale Gas Well Shut-in Period and the Optimization Method of Shut-in Regimen" [grant numbers 52274033].

Data Availability Statement: The authors declare that no copyrighted figures have been used in this manuscript. All data included in this study are available upon request by contacting the corresponding author.

Acknowledgments: We thank the Chongqing Shale Gas Company for providing the experimental samples for this study, and thank Hong Liu of Chongqing University of Science and Technology for his contribution to the development of this research experiment.

Conflicts of Interest: The authors declare no conflicts of interest.

References

1. Wang, S.; Wang, G.; Zeng, L.; Liu, P.; Huang, Y.; Li, S. New method for logging identification of natural fractures in shale reservoirs: The Fengcheng formation of the Mahu Sag, China. *Mar. Pet. Geol.* **2025**, *176*, 107346. [CrossRef]
2. Zhan, S.; Ning, S.; Bao, J.; Wu, J.; Zhang, M.; Cui, J. Comparative study on adsorption behaviors of CH_4/CO_2 and CH_4/H_2S in quartz nanopores from molecular perspectives: Implication for EGR in shale reservoirs. *Colloids Surf. A Physicochem. Eng. Asp.* **2025**, *712*, 136419. [CrossRef]
3. Xie, W.; Fu, X.; Wang, H.; Sun, Y. Adsorption kinetics of water vapor in shale and their dependence on in-situ conditions and the composition of reservoirs. *Geoenergy Sci. Eng.* **2025**, *249*, 213779. [CrossRef]
4. Abelly, E.N.; Yang, F.; Ngata, M.R.; Mwakipunda, G.C.; Shanghvi, E.R. A field study of pore-network systems on the tight shale gas formation through adsorption-desorption technique and mercury intrusion capillary porosimeter: Percolation theory and simulations. *Energy* **2024**, *302*, 131771. [CrossRef]
5. Jiang, Y.; Liu, H.; Liang, T.; Zhou, F.; Xu, Q.; He, C. Impact of water-rock interaction on natural fractures and shale permeabilities under the closure stress. *Geoenergy Sci. Eng.* **2024**, *243*, 213357. [CrossRef]
6. Goral, J.; Panja, P.; Deo, M.; Andrew, M.; Linden, S.; Schwarz, J.-O.; Wiegmann, A. Confinement Effect on Porosity and Permeability of Shales. *Sci. Rep.* **2020**, *10*, 49. [CrossRef] [PubMed]
7. Chang, X.; Lin, S.; Yang, C.; Wang, K.; Liu, S.; Guo, Y. A Critical Review of $ScCO_2$-enhanced Gas Recovery and Geologic Storage in Shale Reservoirs. *Gas Sci. Eng.* **2024**, *125*, 205317. [CrossRef]
8. Zhou, J.; Yang, K.; Tian, S.; Zhou, L.; Xian, X.; Jiang, Y.; Liu, M.; Cai, J. CO_2-water-shale interaction induced shale microstructural alteration. *Fuel* **2020**, *263*, 116642. [CrossRef]
9. Liu, K.; Sheng, J.J. Experimental study of the effect of water-shale interaction on fracture generation and permeability change in shales under stress anisotropy. *J. Nat. Gas Sci. Eng.* **2022**, *100*, 104474. [CrossRef]

10. Phan, T.T.; Vankeuren, A.N.; Hakala, J.A. Role of water–rock interaction in the geochemical evolution of Marcellus Shale produced waters. *Int. J. Coal Geol.* **2018**, *191*, 95–111. [CrossRef]
11. Zhou, J.; Yang, K.; Zhou, L.; Jiang, Y.; Xian, X.; Zhang, C.; Tian, S.; Fan, M.; Lu, Z. Microstructure and mechanical properties alterations in shale treated via CO_2/CO_2-water exposure. *J. Pet. Sci. Eng.* **2021**, *196*, 108088. [CrossRef]
12. Goodman, A.L.; Sanguinito, S.; Tkach, M.K.; Natesakhawat, S.; Kutchko, B.G.; Fazio, J.; Cvetic, P.C. Investigating the role of water on CO_2-Utica Shale interactions for carbon storage and shale gas extraction activities–Evidence for pore scale alterations. *Fuel* **2019**, *242*, 744–755. [CrossRef]
13. Gutiérrez-Aguilar, F.; Jiménez-Barranco, S.; Schaaf, P.; Victoria-Morales, A. Fluid-rock interaction processes in ancient subduction zones evidenced by the high-pressure–low-temperature Acatlán complex, Mexico. *Sci. Rep.* **2025**, *15*, 11848. [CrossRef]
14. John, T.; Klemd, R.; Gao, J.; Garbe-Schönberg, C. Trace-element mobilization in slabs due to non steady-state fluid-rock interaction: Constraints from an eclogite-facies transport vein in blueschist (Tianshan, China). *Lithos* **2008**, *103*, 1–24. [CrossRef]
15. Peacock, S.M.; Christensen, N.I.; Bostock, M.G.; Audet, P. High pore pressures and porosity at 35 km depth in the Cascadia subduction zone. *Geology* **2011**, *39*, 471–474. [CrossRef]
16. Taetz, S.; John, T.; Bröcker, M.; Spandler, C. Fluid–rock interaction and evolution of a high-pressure/low-temperature vein system in eclogite from New Caledonia: Insights into intraslab fluid flow processes. *Contrib. Miner. Pet.* **2016**, *171*, 90. [CrossRef]
17. Jiang, O.; Zheng, X.; Gong, Q.; Wu, H.; Chu, B. Research on mass transfer mechanisms due to short-term water-rock interactions between granite cuttings and alkaline NaCl solution and their patterns. *Geoenergy Sci. Eng.* **2025**, *245*, 213512. [CrossRef]
18. Burnside, N.M.; Westaway, R.; Banks, D.A.; Zimmermann, G.; Hofmann, H.; Boyce, A.J. Rapid water-rock interactions evidenced by hydrochemical evolution of flowback fluid during hydraulic stimulation of a deep geothermal borehole in granodiorite: Pohang, Korea. *Appl. Geochem.* **2019**, *111*, 104445. [CrossRef]
19. Crundwell, F.K. The mechanism of dissolution of the feldspars: Part II dissolution at conditions close to equilibrium. *Hydrometallurgy* **2015**, *151*, 151–162. [CrossRef]
20. Vengosh, A.; Jackson, R.B.; Warner, N.; Darrah, T.H.; Kondash, A.J. A critical review of the risks to water resources from unconventional gas development and hydraulic fracturing in the United States. *Environ. Sci. Technol.* **2014**, *48*, 8334–8348. [CrossRef]
21. Zolfaghari, A.; Holyk, J.; Tang, Y.; Dehghanpour, H.; Bearinger, D. Flowback Chemical Analysis: An Interplay of Shale-Water Interactions. In Proceedings of the SPE Asia Pacific Unconventional Resources Technology Conference, Brisbane, Australia, 28 September 2015. [CrossRef]
22. Lin, B.; Cerato, A.B. Applications of SEM and ESEM in Microstructural Investigation of Shale-Weathered Expansive Soils along Swelling-Shrinkage Cycles. *Eng. Geol.* **2014**, *177*, 66–74. [CrossRef]
23. Yasin, Q.; Liu, B.; Sun, M.; Sohail, G.M.; Ismail, A.; Majdański, M.; Golsanami, N.; Ma, Y.; Fu, X. Automatic pore structure analysis in organic-rich shale using FIB-SEM and attention U-Net. *Fuel* **2024**, *358*, 130161. [CrossRef]
24. Ma, X.; Wang, H.; Zhou, S.; Feng, Z.; Liu, H.; Guo, W. Insights into NMR response characteristics of shales and its application in shale gas reservoir evaluation. *J. Nat. Gas Sci. Eng.* **2020**, *84*, 103674. [CrossRef]
25. Ma, X.; Wang, H.; Zhou, S.; Shi, Z.; Zhang, L. Deep shale gas in China: Geological characteristics and development strategies. *Energy Rep.* **2021**, *7*, 1903–1914. [CrossRef]
26. Zhou, M.; Li, J.; Luo, Z.; Sun, J.; Xu, F.; Jiang, Q.; Deng, H. Impact of water–rock interaction on the pore structures of red-bed soft rock. *Sci. Rep.* **2021**, *11*, 7398. [CrossRef] [PubMed]
27. Chen, S.; Wang, H.; Li, F.; Li, P.; Zhou, T.; Li, N.; Xu, L.; Zhang, J. Classification systems of pore-fractures structures and its effects on fracturing fractures propagation in shale reservoir. *Geoenergy Sci. Eng.* **2025**, *244*, 213409. [CrossRef]
28. Wang, B.; Gao, B.; Wang, L.; Wang, S.; Wu, C.; Zhang, W.; Liu, G. Pore Size Evolutionary Mechanism of Anthracite Induced from Water-Rock Interactions. *ACS Omega* **2025**, *10*, 7635–7647. [CrossRef] [PubMed] [PubMed Central]
29. Zhou, S.; Sun, Q.; Zhang, H.; Meng, H.; Gao, Q.; Zhou, Y. Elemental dissolution characteristics of granite and gabbro under high-temperature water-rock interactions. *Sci. Total Environ.* **2023**, *897*, 165455. [CrossRef]
30. Cheng, Q.; You, L.; Chang, C.; Xie, W.; Hu, H.; Wang, X. Implication of Water-Rock Interaction for Enhancing Shale Gas Production. *Fluid Dyn. Mater. Process.* **2024**, *20*, 1441–1462. [CrossRef]
31. Jia, C.; Hu, J.; Sepehrnoori, K. Numerical Studies of Unstable Fingering Flow in a Water-Oil System. In Proceedings of the SPE Improved Oil Recovery Conference, Tulsa, OK, USA, 22–25 April 2024. [CrossRef]